

Impact of range straggling and multiple scattering on proton therapy of brain, using a slab head phantom

S.B. Jia¹, A.A. Mowlavi^{2,3*}, M.H. Hadizadeh¹, M. Ebrahimi Loushab¹

¹Department of Physics, Ferdowsi University of Mashhad, Mashhad, Iran

²Department of Physics, Hakim Sabzevari University, Sabzevar, Iran

³International Centre for Theoretical physics, Associate Federation Scheme, Medical Physics Field, Trieste, Italy

ABSTRACT

► Original article

*** Corresponding author:**

Dr. Ali Asghar Mowlavi,

Fax: +98 571 4411161

E-mail: amowlavi@hsu.ac.ir

Received: Jan. 2013

Accepted: May 2013

Int. J. Radiat. Res., April 2014;
12(2): 161-167

Background: The advantages of proton beam in radiation therapy- like small lateral scattering as well as absence of exit dose tail in the organs which are after the tumor- make it capable of delivering more treatment doses to the target and much lesser to the critical tissues near it. **Materials and Methods:** In this study, the Monte Carlo MCNPX code has been used to simulate a slab head phantom irradiated by proton pencil beams. The simplified slab has tissue compositions of the ICRU 46, and the necessary data have been taken from *adult male phantom* of MIRD-ORNL family series. **Results:** Suitable energy range of incident proton beams has been estimated in order to have the Bragg peaks inside the brain tissue. Energy straggling or, rather, range straggling, and multiple scattering which affect the lateral broadening of incident beams, have been investigated. **Conclusion:** The results show that the FWHM (Full Wide in Half Maximum) increases more than six times from 1.73 mm to 10.78 mm for the energy range of 50 - 135 MeV. The FWHM values of lateral dose profiles change from 1 mm in 50 MeV to 7.5 mm in 135 MeV, and it has been shown that when a pencil beam is used to irradiate a tissue, the absorbed dose in depth along the central axis does not show a Bragg peak pattern.

Keywords: MCNPX code, proton therapy, slab head phantom, range straggling, multiple scattering.

INTRODUCTION

Nowadays, radiation therapy is one of the three main methods in treatment of local cancers; the other two being surgery and chemotherapy. Photons are the most common type of particles in radiotherapy ⁽¹⁾. Despite major technical developments, the exponential decrease in the number of primary photons remains the main problem due to the nature of photon interactions in the matter. Thus, photons have no well-defined range and their dose profiles diminish exponentially. So, a considerable dose is received by healthy organs, before and after the region of interest. Unlike photons, charged particles have relatively well-defined

penetration range. The dominant mechanism by which charged particles lose their energies is inelastic collision with the atomic electrons; they lose most of their energies near the end of their paths, the so called Bragg peak ⁽²⁾.

Other advantages of charged particles are small lateral scattering as well as absence of exit dose tail in the organs which are after the tumor. These make charged particles capable of delivering more treatment doses to the target and much lesser to the critical tissues near it.

Usage of protons in radiation therapy was first proposed by Robert Wilson at Harvard in 1946 ⁽³⁾. The first patient was treated in 1954 at Lawrence Berkeley Laboratory ⁽⁴⁾.

There are two main methods of delivering

beams of desired shape to the target volume: passive scattering, at which the beam is broadened both laterally and longitudinally using mechanical components, and active scanning technique that fast-steering magnets are used to move the pencil beam sidewise, to cover a same layer of target volume⁽⁵⁾. This can be done on a discrete grid known as spot scanning or by moving the pencil beam in a continuous way, called as raster scanning. By altering the incident energy coming from accelerator or by implementing a proper range degrader it is possible to go from one layer to another^(5,6).

Proton energy losses, which are actually statistical processes, gradually bring the particle to rest. The fluctuation in proton range is called range straggling or energy straggling⁽⁷⁾. The result of this will be the broadening of the Bragg peak^(2, 8). Another significant parameter in radiotherapy is the lateral broadening of incident beam as particle penetrates into the matter. Besides collision interactions, elastic coulomb scatterings also occur off atomic nuclei, but energy losses are negligible. Since in Rutherford scattering the interaction cross section increases with decreasing scattering angle, each elastic coulomb scattering causes a small deviation in particle direction. But, multiple small angle deviations along the proton path, in total, lead to a change in particle directions that result in a visible deviation in primary path. The lateral broadening of beam due to multiple scattering is often called lateral scattering⁽²⁾.

Clinical measurements and calculations on lateral scattering and also energy straggling have often been done for water or soft tissues. For instance, multiple scatterings of 158.6 MeV protons in 14 different materials have been measured by B.Gottschalk *et al.*⁽⁹⁾ Lateral scatterings of photons, protons and carbon ions in water have been compared with each other, and it is realized that carbon ions have a smaller lateral scattering and a smaller range straggling than protons⁽¹⁰⁾. It is well known that multiple scattering is responsible for lateral beam spreading. Biomaterial scatterers have been developed at Harvard Medical School for lateral

beam-broadening purposes⁽¹¹⁾. The lateral dose profiles were simulated with two standard models by Sawakuchi *et al.*: one, implemented in the standard MCNPX version, and one as an algorithm that incorporates large-angle single scattering events of Molière's theory. The spatial distribution of proton beams in water has been compared for these two algorithms⁽¹²⁾. Sawakuchi *et al.* have also suggested the use of suitable models of multiple scattering in Monte Carlo codes to estimate an accurate low dose envelope for low energy beams⁽¹³⁾.

In this research we have studied the impact of incident proton energy on the Bragg peak- width in depth dose profiles, and also on the lateral scattering due to multiple scattering for a slab-head-phantom irradiated by proton pencil beams.

MATERIALS AND METHODS

A simplified head phantom has been modeled. The Monte Carlo simulations are performed using MCNPX code version 2.4 developed at Los Alamos National Laboratory in USA⁽¹⁴⁾. The modeled phantom, up-down, is composed of 0.2 cm of human skin, 0.3 cm of soft tissue, 0.9 cm of cranium, 11.5 cm of brain, 0.9 cm of cranium, and finally 0.5 cm of soft tissue. The geometry used in the simulation is presented in figure 1. Mass densities and compositions of the organs are given in table 1.

Here, the lateral dimensions of the phantom were assumed in accordance with the maximum values of brain dimensions in MIRD-ORNL phantom as 17.2 cm × 13.2 cm. Mono energetic proton pencil beams perpendicular to the layers and toward the bottom of phantom have been used⁽¹⁶⁾.

Using rectangular mesh grids on geometry of slab head phantom, we have obtained the depth and the lateral dose profiles. Two different mesh grids were used to do the calculations: first, grids of thickness 0.1 mm and lateral dimensions of the tissue all over the organ; and second, one of the aforementioned grids laterally cut into layers of 0.5 mm and placed at a specific depth.

Table 1. Mass density and elemental composition of the tissues in the head phantom (Compositions are expressed as percentage by weight ⁽¹⁵⁾).

Tissue type	Density (g/cm ³)	H	C	N	O	Ca	Na	P	S	Cl	K
Skin	1.09	10	20.4	4.2	64.5	-	0.2	0.1	0.2	0.3	0.1
Soft tissue	1.03	10.5	25.6	2.7	60.2	-	0.1	0.2	0.3	0.2	0.2
Cranium	1.61	5	21.2	4.0	43.5	17.6	0.1	8.1	0.3	-	-
Brain	1.04	10.7	14.5	2.2	71.2	-	0.2	0.4	0.2	0.3	0.2

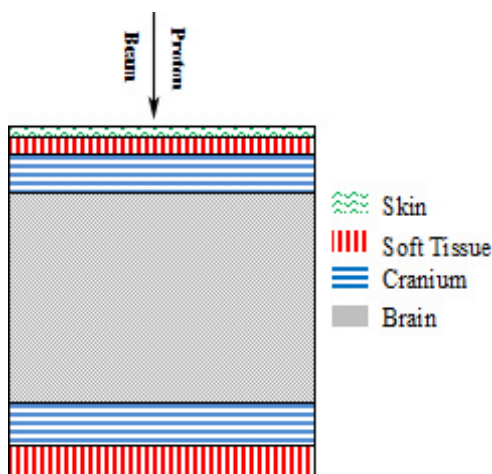


Figure 1. Geometry of the slab head phantom.

RESULTS

Depth dose profiles in the phantom are shown in figure 2 for proton beams with energy ranges of 40 to 160 MeV. As can be seen, the Bragg peaks fall inside the brain for beam energies of 50 to 140 MeV. Depending on the size and location of brain tumors, suitable energies can be chosen according to these profiles. It can be seen that by increasing the incident proton energies, the peaks get wider and shorter which means the range straggling is larger for higher energies, as expected. These can be used for better conformation of dose distribution in shape of targeted tumor.

Depth dose profiles analysis

In figures 3–5, Bragg peak positions, proton beam ranges in brain, and the FWHM (Full Wide in Half Maximum) of Bragg peaks are shown as functions of proton energy, respectively. In figure 3, the data of Bragg peak positions are well fitted by a second order polynomial function of energy. The experimental well-known Geiger’s

range-energy formula ($R=\alpha E^p$) which is true for a phantom of same medium, does not have a good agreement here ⁽¹⁷⁾. The evaluated constant parameters are also shown. In figure 4, proton- beam ranges are stated in two forms: the 10% and the 90% ranges. These are the distances over which the absorbed dose drops to 0.1 and 0.9 its maximum value.

As can be seen, the 10% and 90% ranges differ by small amounts, and their absolute values increase with energy. For instance, for 130 MeV, the difference is 2.66 mm. Figure 5, illustrates the effect of energy increase on peak-widths. The Bragg-peak FWHM’s vary from about 1.73 mm for 50 MeV, to about 10.78 mm for 135 MeV. Also calculated, are the standard deviations at distal region of depth dose profiles, which are given in table 2. These, play a key role in the quality of the dose-distribution-spread along the depth of the tumor.

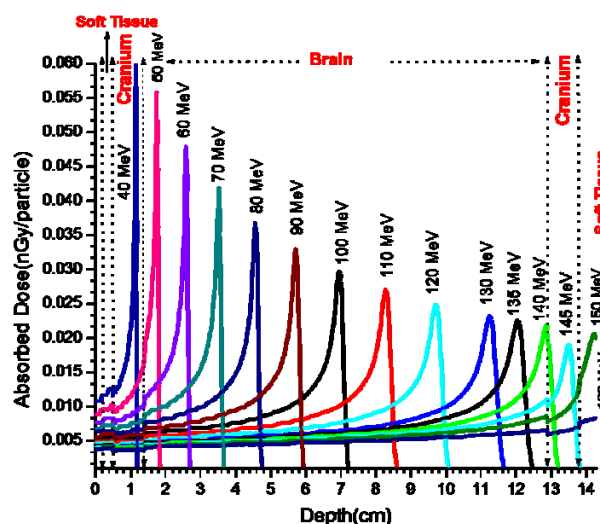


Figure 2. Pristine depth dose profiles in slab head phantom for the incident pencil beams with energies between 40 MeV to 145 MeV.

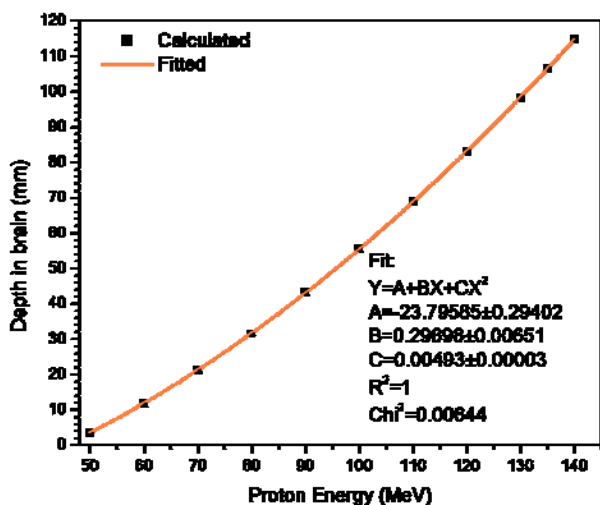


Figure 3. Bragg-peak positions within the brain as a function of energy.

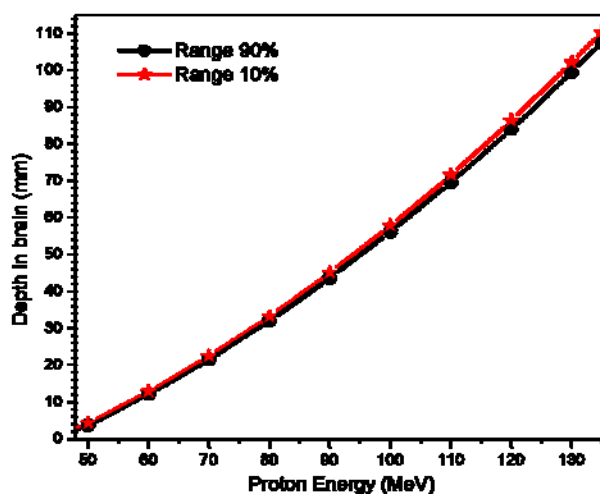


Figure 4. The range of proton beams in the brain for the distal 0.9 and 0.1 dose levels.

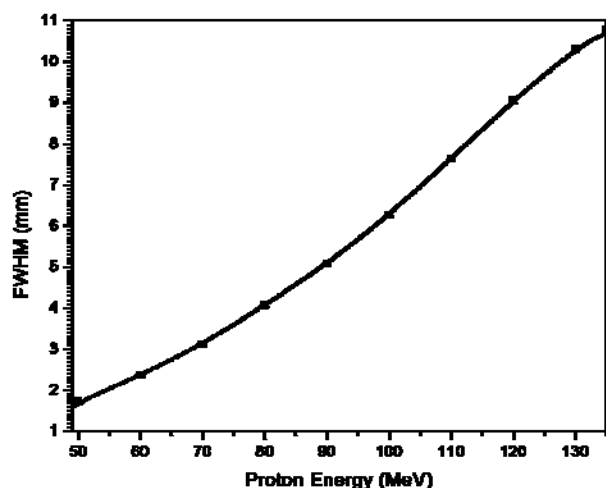


Figure 5. The FWHM values of the Bragg peaks as a function of energy.

Table 2. Standard deviations at distal region in depth dose profiles.

Energy (MeV)	Sigma (mm) in distal region	Energy (MeV)	Sigma (mm) in distal region
50	0.35	100	1.17
60	0.47	110	1.46
70	0.56	120	1.60
80	0.80	130	1.94
90	0.99		

normal organs. From these curves, the FWHM values and the penumbra (80%-20%) have been assessed in the depths corresponding to Bragg peak positions for any beam energy. Results are shown in figures 7 and 8. It is seen that by increasing the proton beam energy, the FWHM and the penumbra increase approximately as a quadratic function, with parameters given in the legends. The FWHM values change from 1 mm at 50 MeV, to 7.5 mm at 135 MeV.

In figure 9, lateral dose profiles are plotted for 100 MeV incident proton beam in various depths of brain. It is seen that the lateral broadening or the lateral scattering, increases with the penetration depth of proton beam.

It is interesting to note from figure 9, the manner in which the maxima of lateral dose profiles change. At the beginning, the peak height in the lateral dose profile declines with depth increase, but the rate of its fall slows down, until, at a specific depth, it starts rising

Multiple scattering

Figure 6 shows the lateral dose profiles in the depth corresponding to the characteristic Bragg peak positions for various incident energies of proton pencil beams. As it can be seen, the dose lateral broadening in depths, corresponding to the positions of dose peaks, increases with energy. The significance of the dose lateral broadening is its effects on the lateral conformity of the dose distribution with the tumor. It determines the amount of lateral beam displacement in spot scanning.

The larger the lateral scattering causes the higher the absorbed dose in the surrounding

again reaching its maximum at the Bragg peak. For the smaller lateral mesh, which is used to calculate the lateral dose profiles, and also for beams with higher energies, this is more obvious. The cause of this behavior can be attributed to multiple scattering which decreases the number of particles passing along the central axis as the penetration depth increases. The outcome is a drop in absorbed energy. On the other hand, as the depth increases, the stopping power also increases, such that it may compensate the decline in the absorbed energy.

Up until a specific depth, the reduction in the absorbed energy due to the lateral scattering

dominates the increase due to the stopping power. Over this distance, the overall absorbed energy decreases. Thereafter, the role of stopping power on absorbed energy dominates, and, as a result, the absorbed energy increases

To describe the lateral scattering more quantitatively, the FWHM variations, and lateral penumbra (80-20%) are presented in figures 10 and 11 as functions of the penetration depth in brain for proton pencil beams of 70 MeV, 100 MeV and 130 MeV.

In these curves it is seen that at a certain depth, beams with lower energies have more broadening effects, and for lower energy beams the lateral broadening increases with depth

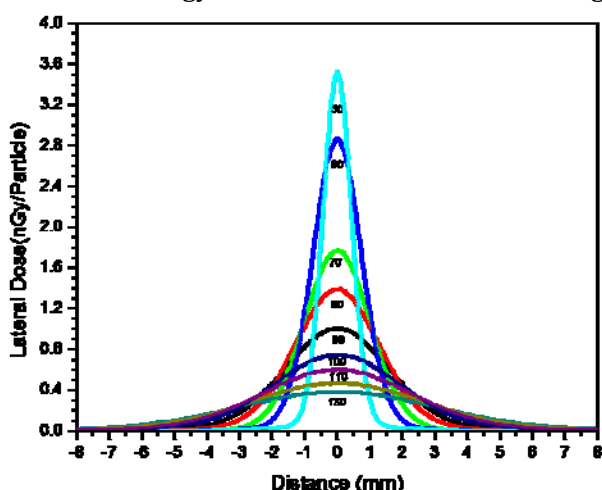


Figure 6. The lateral dose profiles for the proton pencil beams at depths corresponding to Bragg peak positions at different energies.

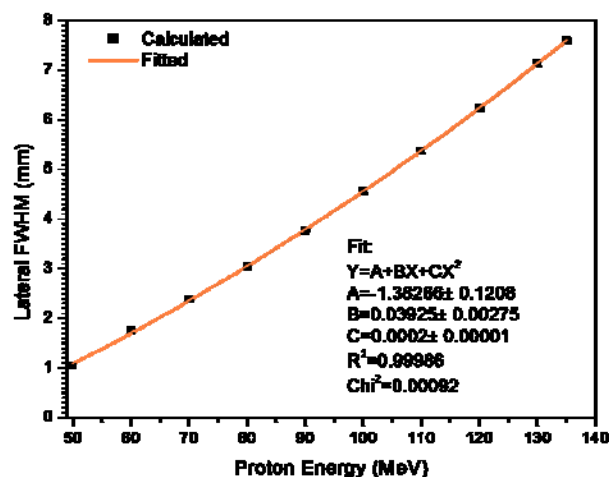


Figure 7. The FWHM values of the lateral dose profiles as a function of energy for proton pencil beams at depths corresponding to Bragg peak positions.

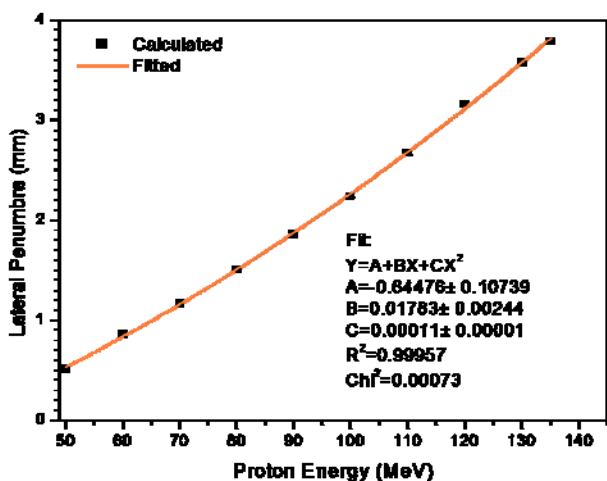


Figure 8. The Penumbra (80-20%) of the lateral dose profiles as a function of energy for proton pencil beams at depths corresponding to the Bragg peak positions.

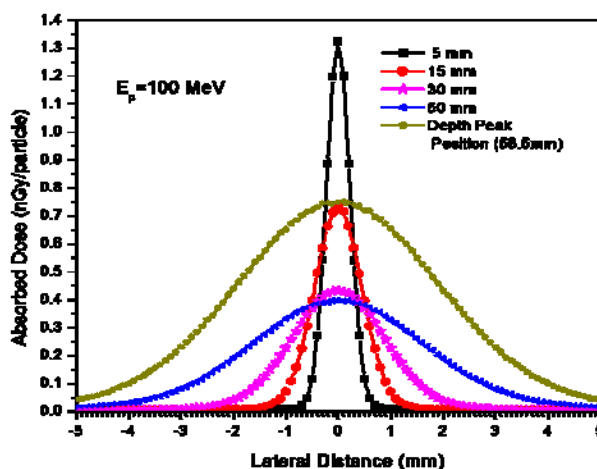


Figure 9. The lateral dose profiles for the proton pencil beam of 100 MeV at various depths.

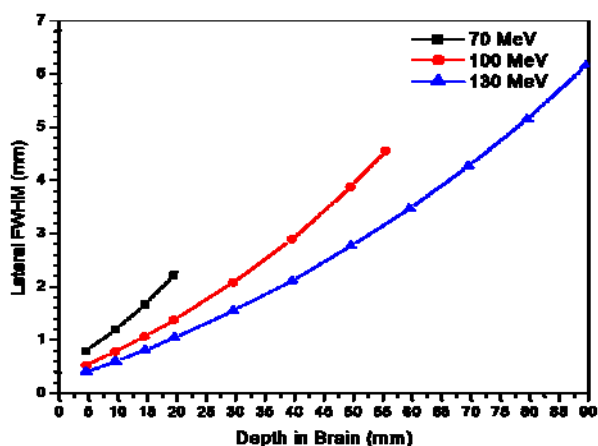


Figure 10. The FWHM values of the lateral dose profiles as a function of the penetration depth in brain for incident pencil beams of 70 MeV, 100 MeV and 130 MeV.

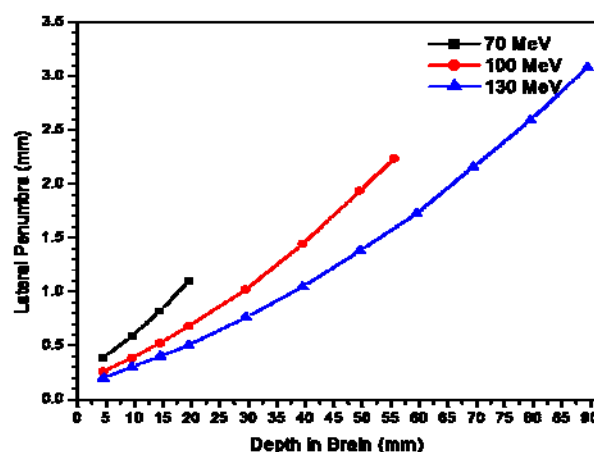


Figure 11. Penumbra (80-20%) of the lateral dose profiles as a function of penetration depth in brain for incident pencil beams of 70, 100, and 130 MeV.

faster. For instance, to penetrate the brain from a depth of 5 to 10 cm, the increases in the FWHM of the lateral dose profiles are 0.41 mm, 0.25 mm and 0.19 mm, for 70, 100, and 130 MeV proton beams, respectively.

DISCUSSION

By using the analytic function that we obtained for the Bragg-peak position against the proton energy (figure 3) suitable energy ranges can be determined according to the size and location of the tumor, in order to spread the Bragg peak over its entire volume. A good knowledge on pristine depth and lateral dose profiles in the target volume is necessary to choose reasonable beam displacement for a good conformation with the shape of the tumor, and much spare of normal tissues⁽¹⁸⁾. Traditionally, most of dose calculations and TPS (treatment planning systems) in hadrontherapy are done in water due to its proximity to soft tissues⁽¹⁹⁾. To be more precise, it would be better to take into account the exact composition and sequence of different tissues⁽²⁰⁾. This, indeed, is the main task of this work. The effects of different tissues along the beam on energy straggling and lateral scattering have been considered for better conformation of dose distribution with tumor shape. Our calculations show that to have a nearly uniform dose

distribution in the tumor region using a typical spot scanning system, the beam displacement, both in traverse and depth, should be linked to the beam energy or, in other words, to the peak position. For example if the center of a typical tumor is placed 2 cm in depth of the brain, corresponding to the peak position of 70 MeV protons, to have a good modulation along the depth, the adjacent layers should be 0.5 mm apart. And if the tumor is located in the depth corresponding to 100 MeV protons, this distance should be 1.2 mm to have uniform SOBP without ripples in dose distribution.

And in a typical spot scanning center, for a laterally uniform dose distribution, the beam spot should be shifted sidewise by an amount proportional to the standard deviation of the lateral dose profiles, which increases by beam energy and, thus, with the depth location of the tumor.⁽²¹⁾ It means that if tumor is seated deeper in brain, one can choose larger displacement both laterally and longitudinally in order to have a good conformation with tumor shape. We can also say that along the central axis, the Bragg peak pattern in depth dose profile disappears if a pencil beam is used to irradiate the target. This phenomenon is known as the “absence of charged particle equilibrium”⁽²¹⁾. If a wide beam is used, this can be avoided to some degree, depending on the beam “width”.

CONCLUSION

We have investigated the effect of energy beam on the proton range straggling and multiple scattering in the slab-head-phantom with the real elemental composition, in this research. For different energy beam, the Bragg peak positions are found in brain phantom and fitted in the second order polynomial function of energy very well. The result shows that by increasing the incident proton energies, the peaks get wider and shorter which means the range straggling is larger for higher energies, as expected. We have also obtained a suitable quadratic fit function for width of lateral dose profiles as a function of energy at a depth corresponding to Bragg peak position. These can be used in a typical spot scanning proton therapy system to adjust the spot displacement both laterally and longitudinally for better conformation of dose distribution in shape of targeted tumor and spare critical tissues near it.

REFERENCES

- Haberer T (2002) Advances in Charged Particles Therapy. Nuclear Physics in 21st Century. Int Nucl Phys Conf INPC 2001. *AIP Conf Proc*, **610**: 157-166.
- Kraft G (2000) Tumor Therapy with Heavy Charged Particles. *Progress in Particle and Nuclear Physics*, **45**: 5473-544.
- Wilson RR (1946) Radiological use of fast protons. *Radiology*, **47**: 487-491.
- Tobias CA, Lawrence JH, Born JL, McCombs R, Roberts JE, Anger HO, Huggins C (1958) Pituitary Irradiation with High Energy Proton Beams: a Preliminary Report. *Cancer Research*, **18**: 121-134.
- Smith AR (2009) Vision 20/20: Proton therapy. *Med Phys*, **36(2)**: 556-568.
- Paganetti H and Bortfeld T (2005) Proton Beam Therapy – The state of the Art, New technologies in radiation oncology. Medical Radiology Series, Springer Verlag, Heidelberg; ISBN3-540-00321-5.
- Bortfeld T (1997) An analytical approximation of the Bragg curve for therapeutic proton beams. *Med Phys*, **24(12)**: 2024-2033.
- Bichsel H, Attix FH, Roesch WC (1968) Charged-particle interactions. In: Radiation Dosimetry. Eds. *Academic Press, New York*. **1**: 157-228.
- Gottschalk B, Koehler AM, Schneider RJ, Sisterson JM, Waner MS (1993) Multiple coulomb scattering of 160 MeV protons. *Nuclear Instruments and methods in physics Research B* **74**: 467-490.
- Weber U (1996) Volumenkonforme Bestrahlung mit Kohlenstoffionen. PhD Thesis, Universitat Gh Kassel.
- Chu WT, Ludewigt BA, Renner TR (1993) Instrumentation for Treatment of Cancer Using Proton and Light-Ion Beams: Review of Scientific instruments, Accelerator & Fusion Research Division, LBL-33403 UC-406.
- Sawakuchi GO, Mirkovic D, Perles LA, Sahoo N, Zhu XR, Ciangaru G, et al. (2010) An MCNPX Monte Carlo model of a discrete spot scanning proton beam therapy nozzle. *Med Phys*, **37(9)**: 4960-4970.
- Sawakuchi GO, Titt U, Mirkovic D, Ciangaru G, Zhu X R, Sahoo N et al. (2010) Monte Carlo investigation of the low-dose envelope from scanned proton pencil beams. *Phys Med Biol*, **55**: 711-721.
- Waters LS, Hendricks J, Kinney GMC (2002) Monte Carlo N-Particle Transport Code system for Multiparticle and High Energy Applications, Los Alamos. NM: Los Alamos National Laboratory.
- White GRDR, Wilson IJ (1992) Photon, Electron, Proton and Neutron Interaction Data for Body Tissues. *ICRU Report 46*. Bethesda, Maryland, USA.
- Eckerman KF, Cristy M, Ryman JC (1996) The ORNL mathematical phantom series. available at: <http://homer.ornl.gov/vlab/mird2.pdf>.
- Evans RD (1982) The atomic nucleus. McGraw-Hill, USA.
- Slopsema R (2011) Beam delivery using passive scattering. In: Proton therapy physics (Ed. Paganetti H); *CRC Press/Taylor & Francis*, 1-18.
- Paganetti H (2009) Dose to water versus dose to medium in proton beam therapy. *Phys Med Biol*, **54**: 4399-4421.
- Torfimov A and Bortfeld T (2003) Beam delivery sequencing for intensity modulated proton therapy. *Phys Med Biol*, **48**: 1321-1331.
- Vatnitsky SM, Miller DW, Moyers MF, Levy RP, Schulte RW, et al. (1999) Dosimetry techniques for narrow proton beam radiosurgery. *Phys Med Biol*, **44**: 2789-2801.

